**4-th International Meeting on**
Cavitation and Dynamic Problems in Hydraulic Machinery and Systems,
October, 26-28, 2011, Belgrade, Serbia

# Procedure for the break-up of cavitation sheet

**Aurélia Vallier[1], Johan Revstedt[1] and Håkan Nilsson[2]**

[1]Fluid Mechanics/Energy Sciences, LTH Lund University

Lund, SE-221 00, Sweden, aurelia.vallier@energy.lth.se, johan.revstedt@enegy.lth.se

[2]Applied Mechanics/Fluid Dynamics, Chalmers University of Technology

Gothenburg, SE-412 96, Sweden, hani@chalmers.se

**Abstract**

The actual mass transfer cavitation models are limited by the grid size dependency of the Volume-Of-Fluid method. A new multi-scale approach is developed which can model the presence of bubbles smaller than the grid size. Using this method for simulations of cavitating hydrofoil will lead to a better modelling of the mixture of vapor and liquid in the transition region between the attached cavity and the shedding cloud. The principle of this approach is to complement the VOF method with a two-way coupling Lagrangian particle tracking method. The VOF-LPT coupling model is tested on simplified configurations for the breakup of an attached cavity. The results show that the model successfully displays the formation of small structures and gives a better description of the liquid/gas mixture.

**Keywords**: numerical simulation, VOF, LPT, multi-scale, cloud cavitation, OpenFOAM.

## 1. Introduction

In the last decade, numerous numerical cavitation models have been developed to describe the mechanisms of the sheet and cloud cavitation on cavitating hydrofoils. A sheet cavity is a steady attached structure which covers a part of the hydrofoil. When the angle of attack is increased or the cavitation number decreased, cloud cavitation occurs which corresponds to foamy and unsteady structures. The cavity length oscillates because the rear part of the cloud is periodically detached from the cavity. The mass transfer models based on a Volume-Of-Fluid (VOF) formulation succeed to represent the attached sheet cavity, the re-entrant jet which breaks the sheet and the shedding of the cloud of vapour (Sauer and Schnerr [1], Kunz *et al.* [2]). However, these models give poor results regarding two aspects:

- The transition between the attached sheet cavity and the cloud of vapour is not resolved. This transition is sharp in simulations (Huuva *et al.* [10]) while experimental observations suggest the presence of vapor and gas bubbles.
- The cloud of vapor which is detached from the sheet cavity doesn't collapse when it comes to the region with higher pressure. It is only transported downstream because the cloud is treated as a incompressible volume of vapor..

Hence, these models are well adapted to flow with separated phases but they fail as soon as cavitation consists of two highly mixed and very unstable phases.

The VOF method is designed to track the interface between two fluids. This method is therefore suitable for modeling large vapor structures, such as sheet cavitation. The drawback of this method is that it cannot describe structures that are smaller than the grid size. A higher resolution grid would be required to capture the small cavitation bubbles which influence the global dynamic of the flow and which are present in the case of cloud cavitation. This would increase excessively the computational cost. For modeling this type of cavitation, the appropriate method is to track individual bubbles in a Lagrangian frame. Furthermore, if the small bubbles dynamics is resolved by a Rayleigh-Plesset equation ( Spång [3]), the collapse of individual bubbles which leads to the global collapse can be modeled. This will give a better understanding and a more accurate prediction of the collapse and its consequences such as pressure wave and pitting on the surface (Grekula [4]).

In order to improve the available cavitation models, we introduce a model that accounts for the entire spectrum of bubble sizes. The VOF and LPT methods are combined within an hybrid approach which uses the strength of the VOF method to model the large structures and the strength of the LPT method to model the small structures.

## 2. Numerical approach

### 2.1 The VOF method for mass transfer cavitation model

The volume of fluid method is a numerical technique for tracking and locating the interface (Hirt and Nichols [7]). It is useful for modeling large vapor structures, therefore it is adapted for modeling sheet cavitation and this method is used in mass transfer cavitation models (Sauer and Schnerr [1], Kunz et *al*. [2]).
The liquid volume fraction α may vary from 0 to 1 within a computational cell. The interface exists in the cells with intermediate values. The mixture density ρ and viscosity μ are calculated using the volume fraction:

$\rho = \alpha \rho_l - (1-\alpha) \rho_g$ (1)
$\mu = \alpha \mu_l - (1-\alpha) \mu_g$ (2)

where the subscript l and g stand for liquid and gas.
The transport equation for the volume fraction reads

$$\frac{\partial \alpha}{\partial t} + \nabla \cdot (\alpha \mathbf{U}) + \nabla \cdot (\alpha(\mathbf{1}-\alpha)\mathbf{U}_\mathbf{r}) = \mathbf{S}_\alpha \qquad (3)$$

where **U** is the velocity of the mixture and $\mathbf{U_r}$ is the relative velocity between the two fluids.
The third term in the l.h.s. of eq. (3) is an extra artificial compression term active only in the interface region. It is introduced by Rusche [8] to preserve the interface sharpness which is crucial in the VOF approach.
In mass transfer cavitation models, the destruction and production of vapor is accounted for by the source term in eq. (3):

$$\mathbf{S}_\alpha = \frac{-\dot{m}}{\rho_g}$$

The mass transfer rate $\dot{m}$ between the liquid and the gas phase depends on the pressure, empirical parameters (Kunz et *al.* [2]) and on the nuclei number and size (Sauer and Schnerr [1]).
Within the context of the VOF method, the mass and momentum equations read

$$\nabla \cdot \mathbf{U} = \mathbf{0} \qquad (4)$$

$$\frac{\partial \rho \mathbf{U}}{\partial t} + \nabla \cdot (\rho \mathbf{U} \otimes \mathbf{U}) = -\nabla p + \mu \nabla^2 \mathbf{U} - \mathbf{S}_{st} + \mathbf{S}_P \qquad (5)$$

where $p$ is the pressure of the mixture. The additional source term $\mathbf{S}_P$ is due to the influence on the flow of the bubbles tracked within the Lagrangian approach and is derived in the next part. The additional source term $\mathbf{S}_{st}$ models the effect of surface tension (Brackbill [9]).

$$\mathbf{S}_{st} = \sigma_{st} \kappa \delta \mathbf{n}$$

where $\delta$ is the Dirac function which insures that the force is only applied at the interface,

$\sigma_{st}$ is the surface tension coefficient,

$\mathbf{n}$ is the normal vector at the interface ( $\mathbf{n} = \nabla\alpha / |\nabla\alpha|$ ) and

κ is the curvature at the interface ( $\kappa = \nabla \mathbf{n}$ ).

Instead of considering the interface as a sharp discontinuity, it is assumed to have a finite thickness which is a smooth transition from one fluid to the other. The dispersion of the surface tension across the transition region is obtained with the gradient of the volume fraction ∇α. Therefore the quality of the interface description depends on the grid size. Hence, capturing small bubbles requires grid refinement which leads to an increased computational effort. An alternative is to model the small bubbles with a Lagrangian Particle Tracking (LPT) method.

### 2.2 The LPT method for small bubbles

The small bubbles are modelled as Lagrangian point particles and are tracked by a LPT method in the fluid flow. This method is relevant for particles much smaller than the grid size such that the source terms from the particle can be approximated as a point source. The recommended particle size is usually ten times smaller than the Lagrangian grid size. Arlov *et a*l. [5] showed that a particle could fill up to 22% of the Lagrangian cell and still satisfies LPT theory.
A particle *P* is defined by the position of its center, $\mathbf{x_P}$, its diameter, $D_p$, its velocity, $\mathbf{U_P}$ and its density, $\rho_P$. Its volume is assumed to be the volume of a sphere $V_p = D_p^3 \pi / 6$ and its mass is $m_p = \rho_P V_p$.

In a Lagrangian frame, the particle position and motion are calculated from the equations

$$\frac{d\mathbf{x_P}}{dt} = \mathbf{U_P} \qquad \text{and} \qquad m_P \frac{d\mathbf{U_P}}{dt} = \sum \mathbf{F}.$$

Several forces are acting on the particle, such as drag force, lift force, added mass, inertia and buoyancy. In this preliminary study, only the drag force is considered for reasons of simplicity.

$$\mathbf{F}_D = m_P \frac{\mathbf{U} - \mathbf{U_P}}{\tau_P}$$

$\tau_P$ is the relaxation time of the particles, i.e. the time it takes for a particle to respond to changes in the local flow velocity

$$\tau_P = \frac{4}{3} \frac{\rho_P D_P}{\rho C_D |\mathbf{U} - \mathbf{U_P}|}$$

The drag coefficient $C_D$ for a spherical particle is derived from experimental data (Clift [11]) and depends on the particle Reynolds number $Re_P = \rho D_p |\mathbf{U}-\mathbf{U}_p| / \mu$.

$C_D = 24/ Re_P$ if $Re_P < 0.1$
$C_D = 24 (1+1/6\ Re_P^{2/3})/ Re_P$ if $0.1 < Re_P < 1000$
$C_D = 0.44$ if $Re_P > 1000$

The force $\mathbf{f_P}$ exerted by a particle on a unit volume of fluid $V_{celli}$ is proportional to the difference in particle momentum between the instant it enters ($t_{in}$) and leaves ($t_{out}$) the control volume $cell_i$ : $\mathbf{f_P} \propto m_p (\mathbf{U_P}(t_{in}) - \mathbf{U_P}(t_{out}))$ .
The additional source term $\mathbf{S_P}$ in the momentum equation (5) is the contribution of this force for each particle $P_k$ which traveled in the control volume $cell_i$ of volume $V_{celli}$.

$$\mathbf{S_P}[cell_i] = \frac{\mathbf{1}}{V_{cell_i}} \sum_k \mathbf{f_{P_k}}$$

### 2.3. Coupling between VOF and LPT

The new multi-scale approach is based on switching model in order to handle the presence of small structures in a mixture of vapor and liquid. The VOF method is complemented with a two-way coupling LPT method which accounts for the small bubbles on a coarser grid.

This multi-scale model requires

- a parameter and a critical value at which the switching between the VOF and LPT methods is activated,
- a strategy to handle the communication between the VOF and LPT methods such that the mass and momentum are conserved.

The criterion parameter for switching method is simply related to the limit grid size for which LPT theory is valid. In other words, bubbles with a size small enough to be tracked by LPT are converted to point particles.

The strategy is inspired from the technique used by Tomar *et al*. [6] to identify small droplet created during the breakup of a turbulent liquid jet in gas. At each time step, the bubbles described in the Eulerian frame are identified with a so called *connected components technique*. It consists of associating the adjacent cells for which the volume fraction meets a given criterion. In the case of bubble break up, the condition is that the volume fraction is below a threshold value $\alpha_{lim}$. The adjacent cells which fulfil this condition are stored together with the number of the bubble (bubbleID) they belong to. The algorithm efficiency is optimized by using a Hash Table which is a table with two parameters, a key and an associated value. Here the key is the cell label and the value is its bubbleID. In this way, it is easy and fast to retrieve data (cell label) because the searching algorithm doesn't use loops which are time consuming.

Once the bubble identification is completed, the bubbles which can be handled in the Lagrangian frame because of their low volume are converted to particles. The position, size and velocity of these particles are deduced from the Eulerian data and the corresponding volume fraction is removed from the VOF calculations. The particles are tracked with the LPT method and the influence of the particles on the flow is taken into account through a source term in the Eulerian momentum equation.

The Lagrangian grid is coarser than the Eulerian grid in order to fulfill the condition of validty of the LPT theory. The Lagrangian grid size is arbitrarily set to be four times as large as the Eulerian grid size in each direction. The maximum volume for the bubble handled by the LPT model is set to be 10% of the Lagrangian cell volume. With these assumptions, the bubbles described by less than 6.4 Eulerian cells are candidates for being handled by the LPT method on the Lagrangian grid. These bubbles are small enough to be considered as spherical due to the surface tension. Therefore their diameter is derived from the equivalent volume of a sphere.

The detailed algorithm of this coupling method implemented with the OpenFOAM C++ library is presented in Figure 1 and is illustrated by a 2D example in Figure 2.

1- Create List L= {cell label / $\alpha<\alpha_{lim}$ }
2- Find connected components:
set maximum bubbleID, maxID=0
create a Hash-Table HT which will contain (cell label, bubbleID)
for all cell_i $\in$ L
create List Ln = {cell label of cell_i 's neighbour }
if none element of Ln is a key of HT
( ie no neighbour is part of a bubble yet)
→ add cell_i's label as a new key in HT, with value bubbleID= maxID
→ maxID++
if one element of Ln (cell_k) is a key of HT
(i.e.only one neighbour is already identified as part of a bubble)
→ get the value bubbleID_k associated to the key cell_k
→ add cell_i's label as a new key in HT, with value bubbleID= bubbleID_k
if several elements of Ln (cell_k, k=1,K; K>1) in Ln are keys in HT
(i.e.several neighbours are already identified as part of a bubble)
→ get the values bubbleID_k, k=1,K associated to the keys cell_k k=1,K
→ find the minimum value minID=min{bubbleID_k, k=1,K}
→ add cell_i's label as a new key in HT, with value bubbleID= minID
→ for all elements of Ln with associated value {bubbleID_k, k=1,K}> minID in HT, change the value to minID in HT (i.e. cell _i connects bubbles together)
3- For each bubble, get its properties
B= {keys (cell label) associated to the same value (bubbleID) in HT}
Evaluate the bubble volume $V_P = \sum_B (\mathbf{1}-\alpha_{cell})V_{cell}$
Evaluate the bubble centroid position $\mathbf{x}_P = \frac{\mathbf{1}}{V_P}\sum_B \mathbf{x}_{cell}(\mathbf{1}-\alpha_{cell})V_{cell}$
Find the lagrangian cell corresponding to the centroid position, get its volume $V_{lag}$
If $V_P<V_{lag}/10$ (i.e. the bubble satisfies the criterion for LPT approach)
→ Evaluate the bubble velocity $\mathbf{U_P} = \frac{\mathbf{1}}{V_P}\sum_B \mathbf{U}_{cell}(\mathbf{1}-\alpha_{cell})V_{cell}$
→ Evaluate the bubble diameter $D_P = (6V_P/\pi)^{1/3}$
→ add the small bubble as a new point particle $P(D_P, \mathbf{x_P}, \mathbf{U_P})$ for the LPT simulation
→ delete the corresponding bubble from the VOF simulation $\alpha_{cell\in B} = 1$

**Fig. 1** Algorithm for the VOF to LPT coupling

The choice of the threshold value $\alpha_{lim}$ for bubble identification determines the degree of precision and the computational cost of the method. A value $\alpha_{lim}$ close to 1 means that almost all the cells are retained for the bubble identification. With a lower threshold value, the cells considered for bubble identification are fewer and therefore the computational time is decreased. On the other hand, neglecting the cells with very low gas content may induce errors for the size and the number of structures identified. Therefore a parameter sensitivity study is conducted and the influence of the threshold value on the bubbles distribution and size is presented in the results part.

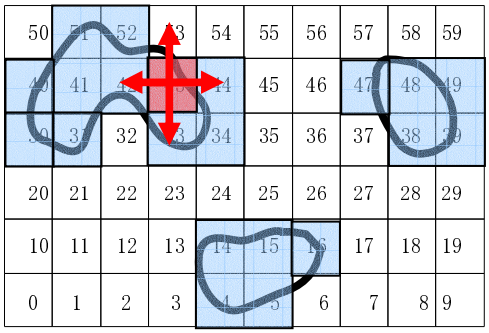


**(a)**

. The cell coloured in blue are identified with $\alpha<0.95$.
. maxID = 0
. The cell labelled 4 has no neighbour in HT therefore the bubble ID 0 is assigned : put HT(4,0), and maxID is set to 1.
. The cell labelled 5 has one neighbour in HT, with bubbleID=0 therefore the bubble ID 0 is also assigned : put HT(5,0)
…
. The cell labelled 30 has no neighbour in HT therefore the bubble ID 1 is assigned : put HT(30,1), and maxID is set to 2.
…
. The cell labelled 33 has no neighbour in HT therefore the bubble ID 2 is assigned : put HT(33,2), and maxID is set to 3.
…
. The cell labelled 43 has two neighbours in HT. The cell 42 with ID=1 and cell 33 with ID=2. Therefore the bubble ID 1 is assigned : put HT(43,1), and the bubble ID of cells 33 and 34 are set to 1.
…

**(b)**

| Key = Label Cell | Value= Bubble ID |
|---|---|
| 4 | 0 |
| 5 | 0 |
| 14 | 0 |
| 15 | 0 |
| 16 | 0 |
| 30 | 1 |
| 33 | 2 |
| 34 | 2 |
| 38 | 3 |
| 39 | 3 |
| 40 | 1 |
| 41 | 1 |
| 42 | 1 |
| 43 | |

| Key = Label Cell | Value= Bubble ID |
|---|---|
| 4 | 0 |
| 5 | 0 |
| 14 | 0 |
| 15 | 0 |
| 16 | 0 |
| 30 | 1 |
| 33 | 1 |
| 34 | 1 |
| 38 | 3 |
| 39 | 3 |
| 40 | 1 |
| 41 | 1 |
| 42 | 1 |
| 43 | 1 |

**(c)**

**Fig. 2** (a) Illustration of the identification of bubbles on a 2D Eulerian grid.

(b) Description of the steps to create the HashTable.

(c) Illustration of the HashTable when a new cell merges two identified bubbles.

## 3. Results

In order to validate the VOF–LPT coupling method for future application to cavitation modeling, numerical simulations of the breakup of an air bubble in water are performed. The geometrical set-up is shown in Figure 3. It consists of a box filled with water and an air bubble staying on the bottom (i.e. no gravity assumption prevents it from rising). The grid and fluid properties are given in Table 1.

The case 1 (Figure 3a) is similar to the set-up for the simulations performed by Gopala *et al.* [12] and the experiments of Andersson and Andersson [13] where a water jet impacts the bubble from above.

In the test case 2, the same grid is used but the inlet is situated under the air bubble (Figure 3b). The direction of the jet velocity is inclined by 30 degrees such that this configuration is a simplified representation of the re-entrant jet which breaks the attached cavity in the context of cloud cavitation.

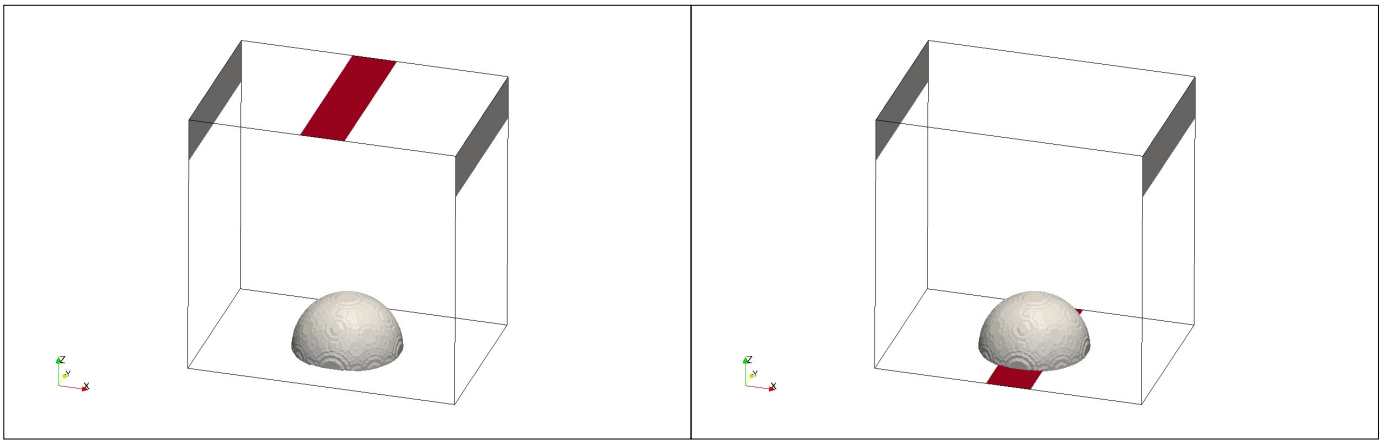

**(a)** **(b)**

**Fig. 3** Geometrical set-up (a) case 1, (b) case 2. Inlet is colored in red, outlet in dark grey and bubble in grey.

| | |
|---|---|
| Density [kg/$m^{-3}$] | $\rho_l = 997$ $\rho_g = 1$ |
| Viscosity [kg/ms] | $\mu_l = 1\,e^{-3}$ $\mu_g = 2\,e^{-5}$ |
| Surface tension | 0.072 |
| Inlet velocity [m/s] | $\|\mathbf{U}\| = 0.5$ |
| Dimensions in (x,y,z) direction [m] | $0.03 \times 0.02 \times 0.03$ |
| Number of cells in (x,y,z) direction | $96 \times 64 \times 96$ |

**Table 1** Physical and grid properties

### 3.1. Case 1

The bubble is stretched under the influence of the jet velocity (Figure 4a). Then the extremities grow and the middle part becomes thinner. Two children bubbles are formed and are linked by a thin strip (Figure 4b). This connecting strip is eventually detached from the two bubbles which continue to move apart from each other. These results are in agreement with both experiments [13] and numerical simulations [12].

In the numerical simulations of Gopala *et al*. [12], the pure VOF method predicted that the connecting strip evolved into two small bubbles. Thanks to the coupling VOF-LPT, the present simulations describe also these two small bubbles and succeed to identify as well a number of smaller bubbles (Figure 5). This shows a gain of accuracy in the modeling of bubble breakup.

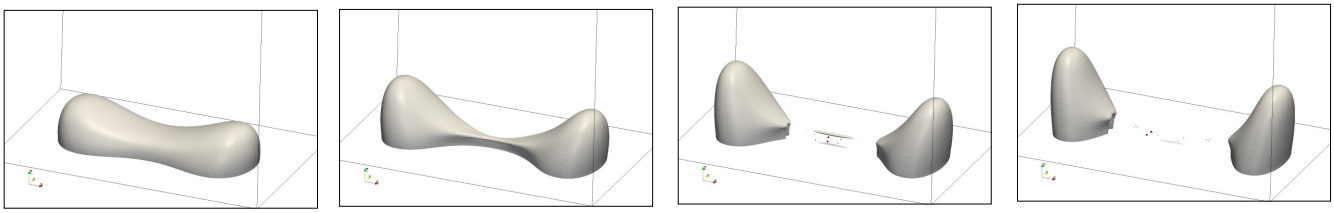

(a) (b) (c) (d)

**Fig. 4** Isosurface $\alpha$=0.5. Instantaneous pictures of the bubble deformation and breakup.

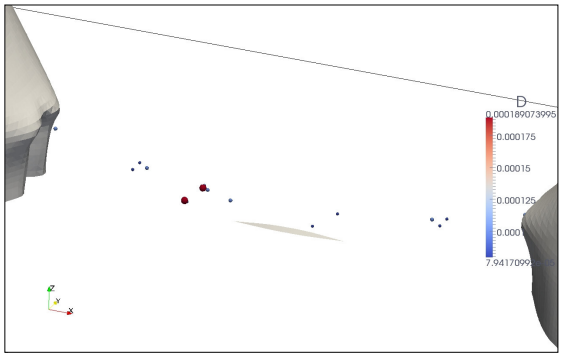


**Fig. 5** Close up of Figure 4d. The two larger bubble are modeled by the VOF method (Isosurface $\alpha$=0.5 colored in grey) and the small bubbles are identified by the coupling method and modeled by the LPT method (colored scaled by the particle diameter).

### 3.2. Case 2

The bubble breakup resulting from a jet impacting the bubble from underneath is illustrated in Figure 6. The presence of small bubbles is successfully captured by the coupling method.

The influence of the value of $\alpha_{lim}$ is studied by comparing the results obtain for $\alpha_{lim}$ =0.95 with the results obtain with $\alpha_{lim}$ =0.9 or 0.99. Figure 7 describes the influence of this parameter on the number of bubbles treated by the LPT method as well as their size. When $\alpha_{lim}$ is increased, the method is more accurate and produces more particles and their sizes are smaller.

With $\alpha_{lim}$ =0.99, the algorithm accounts also for the cells with a lower gas content, i.e. the cells with $\alpha \in [0.95, 0.99[$ are not neglected, compare to the case $\alpha_{lim}$ =0.95. Such a cell is either isolated or adjacent to cells that belong to identified bubbles. In the first scenario, a particle which has a very small diameter is created from this very low volume of gas. In the second scenario, the cell connects several identified bubbles such that the resulting bubble has a volume which doesn't satisfy LPT theory anymore. Therefore the distinct bubbles which were candidates for the LPT approach when $\alpha_{lim}$ =0.95 are now identified as one large bubble which can still be treated by the Eulerian approach.

With $\alpha_{lim}$ =0.9, the cells with a lowest gas content ($\alpha$>0.9) are not accounted for, therefore the smallest bubbles are not detected by the algorithm.

This parameter study highlights the sensitivity of the identification method to the threshold value $\alpha_{lim}$.

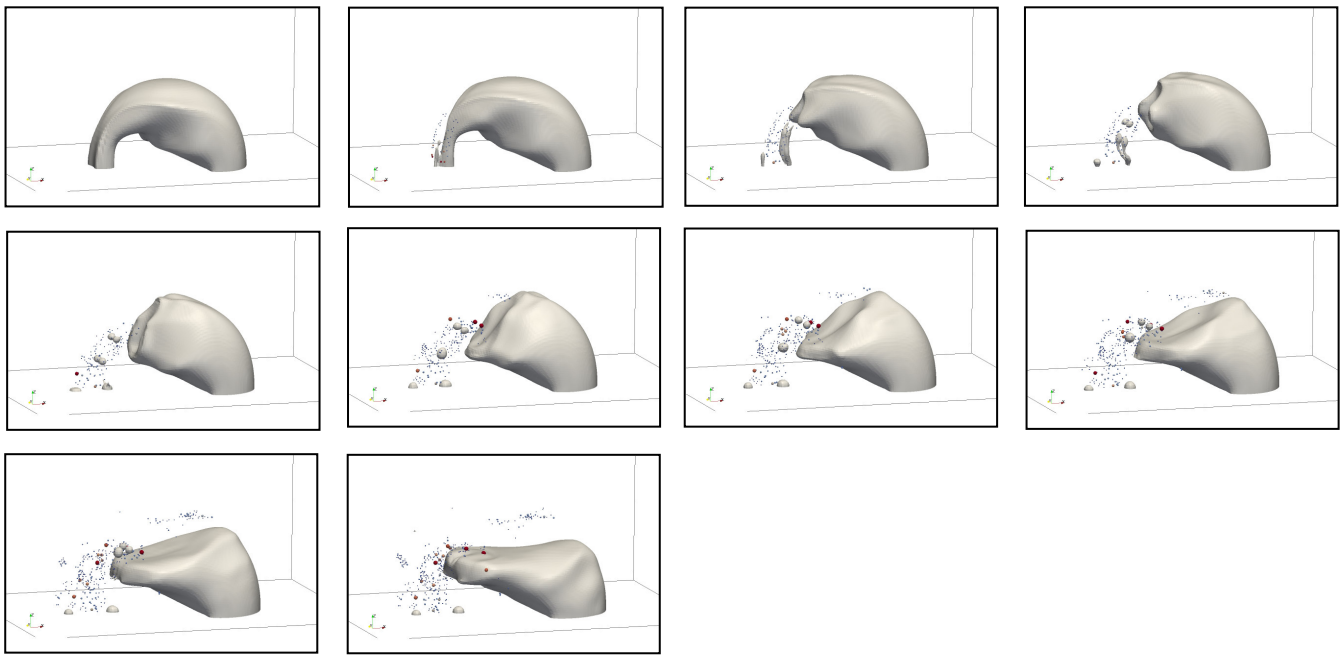

**Fig. 6** Instantaneous picture of the bubble modeled by the VOF method (Isosurface $\alpha$=0.5 colored in grey) and the small bubbles identified by the coupling method and modeled by the LPT method (colored scaled by the particle diameter).

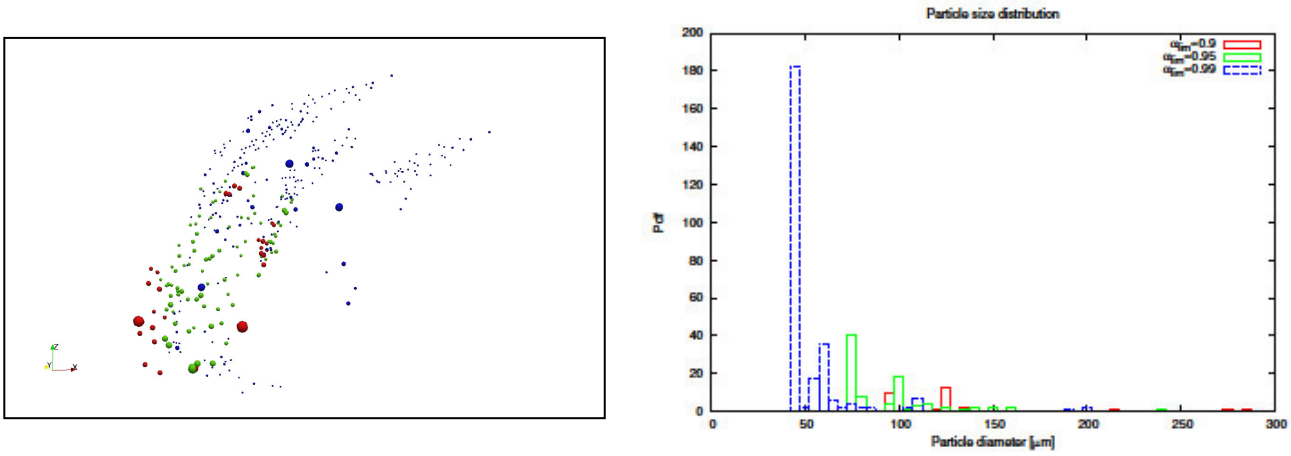


**(a)** **(b)**

**Fig. 7** Size of the particles for different threshold value $\alpha_{lim}$, at t=0.0185. (a) Snapshot of the particles distribution. (b) Probability density function.

## 4. Conclusions

Since a model based on a VOF method fails to describe structures that are smaller than the grid size, it cannot model the small cavitation bubbles without investing an enormous computational effort. These bubbles are present in the case of cloud cavitation and influence the global dynamic of the flow. For this type of cavitation, tracking individual bubbles is more relevant. In order to improve the existing mass transfer cavitation model based on VOF method, a new hybrid method has been developed. This multi-scale approach switches from an Eulerian to a Lagrangian frame in order to account for the small bubbles that a pure VOF method cannot simulate. An algorithm for identifying small bubbles have been implemented in OpenFOAM and the coupling method have been tested on two simple cases of an air bubble breaking up under the impact of a water jet. The second configuration is a

simplified model of the re-entrant jet that breaks the attached cavity in the context of cavitating hydrofoil. The results show the ability of the algorithm to detect small bubbles and track them in the Lagrangian frame. The multi-scale approach is therefore an improvement to the modeling of the transition from sheet to cloud cavitation.

## Acknowledgments

The research presented was carried out as a part of "Swedish Hydropower Center - SVC". SVC has been established by the Swedish Energy Agency, Elforsk and Svenska Kraftnät together with Luleå University of Technology, The Royal Institute of Technology, Chalmers University of technology and Uppsala University. www.svc.nu. I gratefully acknowledge the use of the computing resources of LUNARC, center for scientific and technical computing for research at Lund University. www.lunarc.lu.se.

## Nomenclature

| | |
|---|---|
| $C_D$ | Drag coefficient |
| $D$ | Diameter [m] |
| $F$ | Force [N] |
| $g$ | Gravitational constant [ms$^{-2}$] |
| $m$ | Mass [kg] |
| $p$ | Pressure [Nm$^{-2}$] |
| $Re$ | Reynolds number |
| $t$ | Time [s] |
| $U$ | Velocity [ms$^{-1}$] |
| $V$ | Volume [m$^3$] |

| | |
|---|---|
| $\alpha$ | Volume fraction |
| $\kappa$ | Curvature [m$^{-1}$] |
| $\mu$ | Dynamic viscosity [ kg m$^{-1}$s$^{-1}$] |
| $\rho$ | Density [kg m$^{-3}$] |
| $\sigma$ | Surface tension coefficient [Nm$^{-1}$] |
| | |
| $l$ | Liquid (water) |
| $g$ | Gas (vapor or air) |
| $p$ | Particle |

## References

[1] Sauer J. and Schnerr G.H., 2000, "Unsteady cavitating flow- A new cavitating model based on a modified front capturing method and bubble dynamics", Proceedings of 2000 ASME Fluid Engineering Summer Conference.
[2] Kunz, R.F., Boger, D.A., Stinebring, D.R., Chyczewski, T.S., Lindau, J.W., Gibeling, H.J., Venkateswaran, S., and T.R. Govindan, 2000, "A Preconditioned Navier-Stokes Method for Two-Phase Flows with Application to Cavitation Predication", Computers and Fluids, 29, pp. 849-875.
[3] Spång J., 2008, "Indicating Cavitation Using Bubble Dynamics", MSc. Thesis, Uppsala University, Sweden.
[4] Grekula, M., 2010, "Cavitation Mechanisms related to erosion, Studies on Kaplan turbines, foils and propellers", PhD thesis, Chalmers University of Technology, Sweden.
[5] Arlov D., Revstedt J. and Fuchs L., 2007, "A different approach for handling large bubbles in a square cross-sectioned bubble column combining Large Eddy Simulation with Lagrangian Particle Tracking", 6th International Conference on Multiphase Flow.
[6] Tomar G., Fuster D., Zaleski S. and Popinet S., 2010, "Multiscale simulations of primary atomization", Computers & Fluids, 39(10), pp. 1864-1874.
[7] Hirt, C.W. and Nichols, B.D., 1981, "Volume of Fluid (VOF) Method for the Dynamics of Free Boundaries", J. Comp. Phys., Vol. 39, pp. 201-225.
[8] Rusche H., 2002, "Computational fluid dynamics of diversed two phase flows at high phase fraction", PhD thesis, University of London , England.
[9] Brackbill J.U., Kothe D.B.and Zemach C., 1992, "A continuum Method for Modeling surface Tension", J. Comp. Phys., 100, 335-354.
[10] Huuva T., Cure A., Bark G. and Nilsson H., 2007, "Computations of unsteady cavitating flow on wing profiles using a volume fraction method and mass transfer models", Proceedings of the 2nd IAHR International Meeting of the Workgroup on Cavitation and Dynamical Problems in Hydraulic Machinery and Systems, Scientific Bulletin of the "Polytechnica" University of Timisoara, Romania. Transactions on Mechanics, 52 (66) pp. 21-34.
[11] Clift R., Grace J.R and Weber M.E., 1978, "Bubbles, Drops and Particles", Academic, New York,
[12] Gopala V.R., van Wachem B.G.M. and Andersson B, 2007, "Analysis and Validation of the Breakup of Fluid Particles using Volume of Fluid Method", 6th International Conference on Multiphase Flow.
[13] Andersson, R. and Andersson, B, 2006, "Modeling the breakup of particles in turbulent flows", AIChE Journal, 52(6), pp. 2031-2038